Fast Detection Based on Customized Complex Valued Convolutional Neural Network for Generalized Spatial Modulation Systems

Akram A. Marseet and Taissir Y. Elganimi
Electrical and Electronic Engineering Department, University of Tripoli, Libya
Email: {a.marseet and t.elganimi}@uot.edu.ly

***Abstract*—In this paper, a customized Auto-Encoder Complex Valued Convolutional Neural Network (AE-CV-CNN) that has been developed in a prior work is applied to Single Symbol Generalized Spatial Modulation (SS-GSM) scheme with new extracted features. The achieved reductions in the computational complexity at the receiver is at least 63.64% for M-PSK schemes compared to the complexity of Maximum Likelihood (ML) detection algorithm. This Fast detection algorithm is based on a proposed Low Complexity ML (LC-ML) detector that affords a complexity reduction of at least 40.91%. With these proposed algorithms, the complexity is reduced as the spatial constellation size increases. Furthermore, in comparison to other sub optimal detection algorithms, the computational complexity in terms of real valued multiplications of the AE-CV-CNN applied to LC-ML is independent of the spatial spectrum efficiency which means that the total spectrum efficiency increases with larger spatial constellation size at no additional complexity.**

***Index Terms*—Auto-Encoder Complex-Valued Convolutional Neural Network (AE-CV-CNN), Multiple Input Multiple Output (MIMO), Generalized Spatial Modulation (GSM).**

I. Introduction

The demand for wireless communication services is dramatically increasing [1] due to the application of Internet of things (IoT) [2]. However, the allocated spectrum and the transmission power [3] are limited. Multiple Input Multiple Output (MIMO) transmission is a key technology for current wireless cellular networks such as 4G networks [4]. Long Term Evolution (LTE) is the most efficient spectrum technique for the current MIMO wireless networks. This technique is unable to support data rates at 10 $Gbps$ [5, 6].

The application of neural networks especially the Convolutional Neural Network (CNN) in the physical layer of wireless MIMO systems is getting the interest of researchers. In [7], the authors proposed a novel deep learning model for the physical layer and applied it to Single Input Single Output (SISO) communication systems. They modeled the physical layer as an Auto-Encoder CNN (AE-CNN) model and introduced the concept of Complex Valued Neural Network (CV-NN). However, their model is not applied for MIMO systems. The authors in [8] used an Auto-Encoder Neural Network (AE-NN) in conventional MIMO with full and partial Channel Status Information at the Transmitter (CSIT). The issue of this model is that the use of CSIT consumes more resources (bandwidth, power, and system complexity) at the transmitter and the receiver. In [9], the authors proposed an auto-encoder deep learning detector for the detection of the transmitted signal in Orthogonal Frequency Division Multiplexing (OFDM)-MIMO systems, but with an intensive computational loss function.

The main contributions in this paper are: (i) Developing a novel LC-ML detector that provides an increase in the complexity reduction as the spatial spectrum is increased. (ii) Fast detection using a CNN based model that is developed in [10] and obtaining constant computational complexity in terms of real valued multiplications regardless of the spatial constellation size.

The rest of this paper is organized as follows: Section II includes abstracted introduction to Artificial Neural Network (ANN) and Single Symbol Generalized Spatial Modulation (SS-GSM) schemes. Section III presents the proposed LC-ML and the AE-CV-CNN models. Section IV includes the calculated computational complexities. Section V shows the simulation results of the proposed models, and finally section VI is the conclusion.

II. Artificial Neural Network and Wireless MIMO Systems

A. Artificial Neural Network

The basic building block of ANN is the neuron. The output of the neuron y is expressed as given by (1) [11].

$$y = f\left(\sum_{i=1}^{D} w_i s_i + w_0\right) \tag{1}$$

The inputs $s_1, s_2, ...s_D$ are the input data, $w_1, w_2, ...w_D$ are the learning weights, and $f(.)$ is an activation function.

A simplified CNN consists of three main layers [12]: the convolution layer, the activation function, and the maximum pooling layer. A de-noising Auto-Encoder (AE) is a feed forward CNN that is used for data recovery from a corrupted data [13]. The de-noising AE is generalized as having stochastic encoding function $\mathbf{C}(\mathbf{h}/\mathbf{x})$ applied to the input data $\mathbf{x}$ to produce a corrupted data z, and the de-encoder will reproduce $\hat{\mathbf{x}}$ as close as much to the original data as shown in Figure 1.

The optimal de-noising AE minimizes the loss function as given in Equation (2) [14].

$$L_{min} = ||\hat{\mathbf{x}} - \mathbf{x}||^2 \tag{2}$$

978-1-7281-4352-1/19/$31.00 2019 IEEE

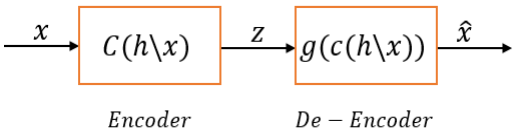

Fig. 1. Block Diagram of De-noising AE.

B. Single Symbol Generalized Spatial Modulation Systems

SS-GSM scheme is based on using $N_a < N_t$ active antennas for each transmission. In SS-GSM, the same symbol is transmitted from all active antennas at the highest spectrum and energy efficiencies.

The spatial constellation size of GSM is given by (3):

$$N_c = 2^{\lfloor log_2 \binom{N_t}{N_a} \rfloor} \tag{3}$$

For MIMO systems with N_t transmit antennas and N_r receive antennas, the received signal vector $\mathbf{r}$ at the input of the receiver is given by (4) [15]:

$$\mathbf{r} = \mathbf{H}_j \mathbf{s}_q + \mathbf{n} \tag{4}$$

where $\mathbf{s}_q \in \mathbb{C}^{N_a \times 1}$ is the transmitted signal vector defined in [10], $q = 1, 2, 3, ..., M$; M is the modulation size, $\mathbf{H}_j \in \mathbb{C}^{N_r \times N_a}$, $j = 1, 2, \ldots, N_c$ is the spatial channel index, and $\mathbf{n} \in \mathbb{C}^{N_r \times 1}$ is an AWGN vector. The elements of $\mathbf{H}_j$ and $\mathbf{n}$ $\sim \mathbb{C}N(0, 1)$.

$\mathbf{H}_j \subset \mathbf{H}$ where $\mathbf{H}$ is the MIMO channel matrix as follows:

$$H = \begin{bmatrix} h_{11} & h_{12} & \ldots & h_{1N_t} \\ h_{21} & h_{22} & \ldots & h_{2N_t} \\ \vdots & \vdots & \ddots & \vdots \\ h_{N_r1} & h_{N_r2} & \ldots & h_{N_rN_t} \end{bmatrix} \tag{5}$$

For simplicity, the term $\sum_{k=1}^{N_a} \mathbf{H}_j(:, k)$ is defined as $\mathbf{h}_j$ as the spatial channel vector.

The received signal at the i^{th} receiver antenna is given by:

$$r_i = \sum_{j=1}^{N_t} h_{ij} x_i + n_i \tag{6}$$

It is clear that (6) represents the argument of the activation function of (1).

The traditional ML detector is given by (7) [16].

$$[j, q] = \underset{\substack{j=1\ldots,N_c \\ q=1\ldots,M}}{\arg\min} ||\mathbf{r} - \mathbf{h}_j s_q||^2 \tag{7}$$

The computational complexity in terms of the number of floating point operations $(C_{ML-T})_{flops}$ and in terms of real valued multiplications $(C_{ML-T})_{rvm}$ of the ML detector of (7) are given in (8) and (9), respectively.

$$(C_{ML-T})_{flops} = 11 N_r N_c M \tag{8}$$

$$(C_{ML-T})_{rvm} = 6 N_r N_c M \tag{9}$$

III. Proposed Model

Based on the proposed model in [10], the explanation of this model is started in this section from the receiver correlation layer at the receiver side.

A. Receiver Correlation Layer

Receiver correlation is basically used to extract the in-phase and quadrature components of the received signals $\mathbf{r}$ of (4).

B. Features Extraction Layer

1) Learning Weights: The estimation of the channel coefficients is equivalent to training the model. This is accomplished through the transmission of pilot symbol which is known to the receiver, and it is given by (10).

$$\mathbf{h}_j = \frac{s^* \mathbf{r}}{|s|^2} \tag{10}$$

Therefore, the estimated channel coefficients represent the learning weights $(w_1, ...w_D)$ of (1).

2) Traditional Features Extraction Algorithm: The extracted features of the traditional ML detector for SS-GSM is given by (11).

$$\mathbf{F}_T = \mathbf{r} - \mathbf{h}_j s_q \tag{11}$$

3) Proposed Features Extraction Method: The proposed features extraction algorithm for SS-GSM is given by (12).

$$\mathbf{F}_P = \frac{s_q^* \mathbf{r}}{|s_q|^2} - \mathbf{h}_j \tag{12}$$

The extracted features of (11) and (12) represent a complex valued errors. The output of this layer is 3D with the dimension of $N_r \times N_c \times M$. From machine learning perspective, M represents the number of modulation classes while N_c represents the number of spatial classes.

From (12), the ML detection of the proposed features extraction is given by (13).

$$[(j, q)_{LC-ML}]_P = \underset{\substack{j=1\ldots,N_c \\ q=1\ldots,M}}{\arg\min} ||\frac{s_q^* \mathbf{r}}{|s_q|^2} - \mathbf{h}_j||^2 \tag{13}$$

C. Activation Function

The absolute value is the activation function which is applied to in-phase component and the quadrature phase component of the extracted features of (11) or (12) separately. In the ideal case, these absolute values have to be zeros. The output of this layer is still a 3D space with a dimension of $N_r \times N_c \times M$.

D. Maximum Pooling

The output space of this layer has a dimension of $N_c \times M$ as it selects the maximum error of the received signals.

E. Loss Function

The loss function of (11) is given in (14):

$$L_T = \max\left(\left|\Re\left(\mathbf{r} - \mathbf{h}_j s_q\right)\right|\right) + \max\left(\left|\Im\left(\mathbf{r} - \mathbf{h}_j s_q\right)\right|\right) \quad (14)$$

The loss function of (12) is given by (15):

$$L_P = \max\left(\left|\Re\left(\frac{s_q^* \mathbf{r}}{|s_q|^2} - \mathbf{h}_j\right)\right|\right) + \max\left(\left|\Im\left(\frac{s_q^* \mathbf{r}}{|s_q|^2} - \mathbf{h}_j\right)\right|\right) \quad (15)$$

F. Classification Layer

The classification layer will estimate jointly the index of the spatial channel matrix $\hat{j}$ and the index of the symbol $\hat{q}$ that minimize (14) or (15) as given in (16) and (17), respectively.

$$[\hat{j}, \hat{q}]_{CNN-T} = \underset{\substack{j=1\ldots,N_c \\ q=1\ldots,M}}{\arg\min} \left[\max\left(\left|\Re\left(\mathbf{r} - \mathbf{h}_j s_q\right)\right|\right) + \max\left(\left|\Im\left(\mathbf{r} - \mathbf{h}_j s_q\right)\right|\right)\right] \quad (16)$$

$$[\hat{j}, \hat{q}]_{CNN-P} = \underset{\substack{j=1\ldots,N_c \\ q=1\ldots,M}}{\arg\min} \left[\max\left(\left|\Re\left(\frac{s_q^* \mathbf{r}}{|s_q|^2} - \mathbf{h}_j\right)\right|\right) + \max\left(\left|\Im\left(\frac{s_q^* \mathbf{r}}{|s_q|^2} - \mathbf{h}_j\right)\right|\right)\right] \quad (17)$$

IV. Computational Complexity

A. Floating Point Operations (flops)

The computational complexity in terms of (*flops*) of the proposed ML detector of (13) is given by (18).

$$\left(C_{ML-P}\right)_{flops} = \left(6 + 5N_c\right) N_r M \quad (18)$$

The computational complexity of (16) in terms of (*flops*) is $\left(C_{CNN-T}\right)_{flops}$ and given by (19), while the computational complexity of (17) in terms of (*flops*) is $\left(C_{CNN-P}\right)_{flops}$ and given by (20).

$$\left(C_{CNN-T}\right)_{flops} = \left(8N_r + 1\right) N_c M \quad (19)$$

$$\left(C_{CNN-P}\right)_{flops} = 6N_r M + \left(2N_r + 1\right) N_c M \quad (20)$$

B. Real Valued Multiplications (rvm)

The computational complexity of (13) in terms of (*rvm*) is $\left(C_{ML-P}\right)_{rvm}$ and given by (21). The complexity of (16) is $\left(C_{CNN-T}\right)_{rvm}$ and given by (22). For (17), the complexity in terms of (*rvm*) is $\left(C_{CNN-P}\right)_{rvm}$ and given by (23).

$$\left(C_{ML-P}\right)_{rvm} = 2(2 + N_c) N_r M \quad (21)$$

$$\left(C_{CNN-T}\right)_{rvm} = 4N_r N_c M \quad (22)$$

$$\left(C_{CNN-P}\right)_{rvm} = 4N_r M \quad (23)$$

V. Results

Numerical calculations for the complexity reductions of (18), (19) and (20) relative to (8) are illustrated in Table I. It is clear that the reduction ratio of both the proposed LC-ML detector and CNN based model increases as the spatial size increases with respect to the computational complexity of the traditional ML detector.

TABLE I
Complexity Reduction Ratio: $M = 8$ and $N_r = 2$.

N_c	$\left(1 - \frac{Eq.19}{Eq.8}\right)\%$	$\left(1 - \frac{Eq.18}{Eq.8}\right)\%$	$\left(1 - \frac{Eq.20}{Eq.8}\right)\%$
4	22.73%	40.91%	63.64%
8	22.73%	47.73%	70.45%
16	22.73%	51.14%	73.86%
32	22.73%	52.84%	75.57%
64	22.73%	53.69%	76.42%

Figure 2 shows the complexity in terms of (*rvm*) of (9), (21), (22) and (23), and compared to the algorithms that presented in [17] and [18] with $N_r = 2$ and $M = 8$. As shown in this figure, the proposed CNN model applied to the proposed LC-ML detector offers the lowest computational complexity, and as a result, the highest total spectrum efficiency.

In Figure 3, the spatial confusion matrix of the proposed CNN model that defined in (17) is shown. In addition, the systems accuracy versus the Signal-to-Noise Ratio (SNR) of SS-GSM over Rayleigh fading channel with $N_t = 5$, $N_r = 2$, $N_a = 2$ and employing 8-PSK technique are shown in Figure 4. It is clear from this figure that the system performance of the proposed CNN based model at the SNR of 16 dB is very close to the performance of the optimal detectors with the advantage of the fast detection.

VI. Conclusion

In this paper, both a new low complexity ML and a fast CNN based detectors are developed for the detection of the transmitted information for M-PSK Generalized Spatial Modulation schemes. Simulation results demonstrated that the CNN based model affords the fastest detection algorithm with low complexity. However, low computational complexity results in low transmission latency. This makes the proposed approach applicable to 5G networks as they heavily rely on massive number of antennas at the base stations. In addition to the fast detection process which increases the total spectrum efficiency, the power consumption is decreased which yields to increasing the total energy efficiency. In the future, this work will be extended to M-QAM scheme.

Appendix

A. Proof of Equation (13)

Equation (7) can be written as follows:

$$[j, q] = \underset{\substack{j=1\ldots,N_c \\ q=1\ldots,M}}{\arg\min} \sum_{i=1}^{N_r} \left[r_i - \left(h_i\right)_j s_q\right] \left[r_i - \left(h_i\right)_j s_q\right]^*$$

$$= \underset{\substack{j=1\ldots,N_c \\ q=1\ldots,M}}{\arg\min} \sum_{i=1}^{N_r} \left[r_i - \left(h_i\right)_j s_q\right] \left[\left(r_i^* - \left(h_i\right)_j^* s_q^*\right)\right] \quad (24)$$

Multiplying the term $\left[r_i - \left(h_i\right)_j s_q\right]$ by $\frac{s_q^*}{|s_q|^2}|s_q|$ and $\left[\left(r_i^* - \left(h_i\right)_j^* s_q^*\right)\right]$ by $\frac{s_q}{|s_q|^2}|s_q|$ yields to:

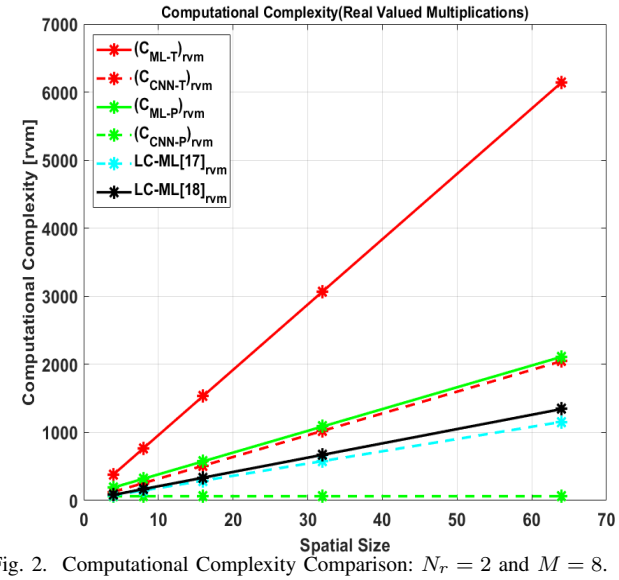

Fig. 2. Computational Complexity Comparison: $N_r = 2$ and $M = 8$.

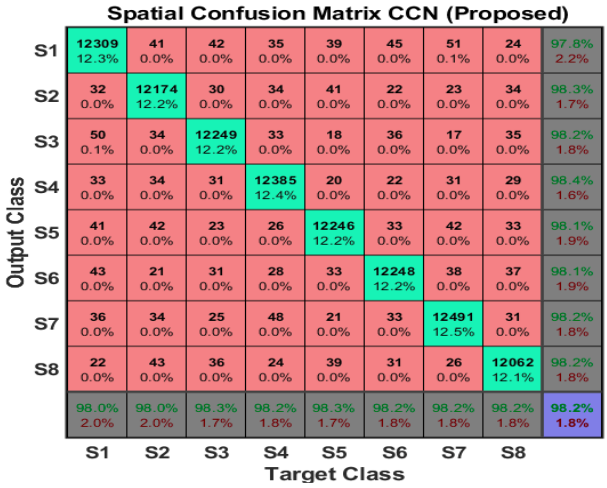

Fig. 3. Spatial Confusion Matrices of Equation (17).

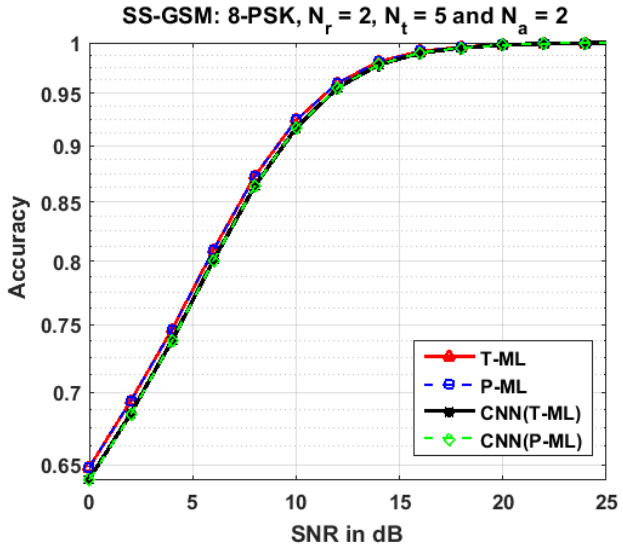

Fig. 4. SS-GSM System Accuracy.

$$
\begin{aligned}
[j,q] &= \underset{\substack{j=1\ldots,N_c\\ q=1\ldots,M}}{\arg\min} \sum_{i=1}^{N_r} \left[\frac{s_q^* r_i}{|s_q|^2} - (h_i)_j\right] \left[\frac{s_q r_i^*}{|s_q|^2} - (h_i)_j^*\right] |s_q|^2 \\
&= \underset{\substack{j=1\ldots,N_c\\ q=1\ldots,M}}{\arg\min} \sum_{i=1}^{N_r} \left[\frac{s_q^* r_i}{|s_q|^2} - (h_i)_j\right] \left[\frac{s_q^* r_i}{|s_q|^2} - (h_i)_j\right]^* |s_q|^2 \\
&= \underset{\substack{j=1\ldots,N_c\\ q=1\ldots,M}}{\arg\min} \sum_{i=1}^{N_r} \left\| \left(\frac{s_q^* r_i}{|s_q|^2} - (h_i)_j\right) \right\|^2 |s_q|^2
\end{aligned}
\tag{25}
$$

The term $|s_q|^2$ is constant and can be neglected to obtain (13) as shown in (26):

$$
[(\hat{j},\ \hat{q})_{LC-ML}]_P = \underset{\substack{j=1\ldots,N_c\\ q=1\ldots,M}}{\arg\min} \sum_{i=1}^{N_r} \left\| \left(\frac{s_q^* r_i}{|s_q|^2} - (h_i)_j\right) \right\|^2 \tag{26}
$$

B. Proofs of (18), (20), (21) and (23)

To determine the computational complexities of (13) and (17), the number of multiplications and summations are as follows:

- *Step (1)*: The term $\frac{s_q^*}{|s_q|^2}$ does not cost any process because it is calculated once before starting the detection process and stored in a memory.
- *Step (2)*: The term $\frac{s_q^* r_i}{|s_q|^2}$, $i = 1\ldots, N_r$ has $4N_rM$ real multiplications and $2N_rM$ summations, and they are independent on the spatial constellation.
- *Step (3)*: The term $\frac{s_q^* r_i}{|s_q|^2} - (h_i)_j$ has $2N_rN_cM$ summations which are dependent on the spatial constellation.
- *Step (4)*: The term $\left|\frac{s_q^* r_i}{|s_q|^2} - (h_i)_j\right|^2$ has $2N_rN_cM$ real multiplications and N_rN_cM summations.
- *Step (5)*: The two terms $\max\left(|\Re\left(\frac{s_q^* \mathbf{r}}{|s_q|^2} - h_j\right)|\right)$ and $\max\left(|\Im\left(\frac{s_q^* \mathbf{r}}{|s_q|^2} - h_j\right)|\right)$ have $4N_rM$ real multiplications, $2N_rM$ summations (from step 2), $2N_rN_cM$ summations (from step 3), and N_cM summations (the sum of $[\max(|\Re(.)|) + \max(|\Im(.)|)]$).

1) Proof of (18): The computational complexity of the proposed model given in (13) is the sum of the calculated complexities (multiplications and summations) in steps 2, 3 and 4 after multiplying by the spatial constellation size N_c, and the result is the same as given in (18); $(6 + 5N_c)N_rM$.

2) Proof of (20): The computational complexity of the proposed AE-CV-CNN of (17) in terms of (*flops*) is calculated as explained in step 5 as follows: $(4N_rM + 2N_rM + 2N_rN_cM + N_cM = 6N_rM + (2N_r + 1)N_cM$.

3) Proof of (21): The computational complexity in terms of (*rvm*) of the proposed LC-ML detector given in (13) is calculated as follows: $4N_rM$ rvms as calculated in step 2 plus $2N_rN_cM$ multiplications as calculated in step 4. Therefore, the rvms complexity of (13) is $2(2 + N_c)N_rM$.

4) Proof of (23): The computational complexity in terms of (*rvm*) of the proposed AE-CV-CNN with the proposed LC-ML detector given in (17) is calculated as follows: $4N_rM$ rvms only, and it is independent on the size of the spatial constellation.

REFERENCES

[1] K. Xiao, F. Wang, H. Rutagemwa, K. Michel and B. Rong, "High-Performance Multicast Services in 5G Big Data Network with Massive MIMO," 2017 IEEE International Conference on Communications (ICC), Paris, 21-25 May 2017.

[2] R. I. Ansari, C. Chrysostomou, S. A. Hassan, M. Guizani, S. Mumtaz, J. Rodriguez and J. Rodrigues, "5G D2D Networks: Techniques, Challenges, and Future Prospects," IEEE Systems Journal, vol. 12, no. 4, pp. 3970-3984, Dec. 2018.

[3] J. Akhtman and L. Hanzo, "Power Versus Bandwidth-Efficiency in Wireless Communications: The Economic Perspective," 2009 IEEE 70th Vehicular Technology Conference Fall, Anchorage, AK, USA, 20-23 Sept. 2009.

[4] R. Hussain, A. T. Alreshaid, S. K. Podilchak and M. S. Sharawi, "Compact 4G MIMO Antenna Integrated with a 5G Array for Current and Future Mobile Handsets," IET Microwaves, Antennas and Propagation, vol. 11, no. 2, pp. 271-279, 1 29 2017.

[5] Q. Ma, P. Yang, P. Wang, L. Peng, X. He, B. Fu and Y. Xiao, "Power Allocation for OFDM with Index Modulation," 2017 IEEE 85th Vehicular Technology Conference (VTC Spring), Sydney, NSW, Australia, 4-7 June 2017.

[6] M. Agiwal, A. Roy and N. Saxena, "Next Generation 5G Wireless Networks: A Comprehensive Survey," IEEE Communications Surveys and Tutorials, vol. 18, no. 3, pp. 1617-1655, third quarter 2016.

[7] T. OShea and J. Hoydis, "An Introduction to Deep Learning for the Physical Layer," IEEE Transactions on Cognitive Communications and Networking, vol. 3, no. 4, pp. 563-575, Dec. 2017.

[8] T. J. OShea, T. Erpek and T. C. Clancy, "Deep Learning Based MIMO Communications," Available at: https://arxiv.org/abs/1707.07980, 2017.

[9] X. Yan, F. Long, J. Wang, N. Fu, W. Ou and B. Liu, "Signal Detection of MIMO-OFDM System Based on Auto Encoder and Extreme Learning Machine," 2017 International Joint Conference on Neural Networks (IJCNN), Anchorage, AK, USA, pp. 1602-1606, 14-19 May 2017.

[10] A. Marseet and F. Sahin, "Application of Complex-Valued Convolutional Neural Network for Next Generation Wireless Networks," 2017 IEEE Western New York Image and Signal Processing Workshop (WNYISPW), Rochester, NY, USA, 2017.

[11] K. L. Moore, "Artificial Neural Networks," in IEEE Potentials, vol. 11, no. 1, pp. 23-28, Feb. 1992.

[12] A. R. Sharma and P. Kaushik, "Literature Survey of Statistical, Deep and Reinforcement Learning in Natural Language Processing," 2017 International Conference on Computing, Communication and Automation (ICCCA), Greater Noida, India, May 2017.

[13] V. A. Knyaz, O. Vygolov, V. V. Kniaz, Y. Vizilter, V. Gorbatsevich, T. Luhmann and N. Conen, "Deep Learning of Convolutional Auto-Encoder for Image Matching and 3D Object Reconstruction in the Infrared Range," 2017 IEEE International Conference on Computer Vision Workshops (ICCVW), Venice, 2017.

[14] Y. Ding, X. Zhang and J. Tang, "Autoencoders," in Deep Learning, MIT Press, 2016.

[15] R. Mesleh, H. Haas, C. W. Ahn and S. Yun, "Spatial Modulation - A New Low Complexity Spectral Efficiency Enhancing Technique," 2006 First International Conference on Communications and Networking in China, Beijing, 2006.

[16] A. Younis, N. Serafimovski, R. Mesleh and H. Haas, "Generalised Spatial Modulation," 2010 Conference Record of the Forty Fourth Asilomar Conference on Signals, Systems and Computers, Pacific Grove, CA, USA, 2010.

[17] C. Lin, W. Wu and C. Liu, "Low-Complexity ML Detectors for Generalized Spatial Modulation Systems," IEEE Transactions on Communications, vol. 63, no. 11, pp. 4214-4230, Nov. 2015.

[18] J. Wang, S. Jia and J. Song, "Signal Vector Based Detection Scheme for Spatial Modulation," IEEE Communications Letter, vol. 16, no. 1, pp. 19-21, Jan. 2012.